Joint Spatial-Temporal Transmission With OFDM Waveforms and Receive Adaptive Filter Design for MIMO Radar-Communications

Xiaonan Xu, Yongzhe Li, Ran Tao, and Tao Shan

School of Information and Electronics, Beijing Institute of Technology, 100081 Beijing, China
Emails: xiaonan.xu@bit.edu.cn, lyz@ieee.org, rantao@bit.edu.cn, shantao@bit.edu.cn

***Abstract*—This paper focuses on the joint transmit and receive design for MIMO radar-communications with orthogonal frequency division multiplexing (OFDM) waveforms. The main objective of this joint design is to seek a maximum signal-to-interference-plus-noise ratio (SINR) at receiver from the radar side, and meanwhile, to guarantee accurate information embedding (IE) performance via OFDM transmission with controlled peak-to-mean envelope power ratio (PMEPR) from the communication side. To achieve this goal, we start from building an appropriate model that incorporates all subcarrier-related characteristics of multi-OFDM waveforms. Based on this model, we formulate the design as a non-convex optimization problem. The objective function therein corresponds to the output SINR, while the constraints include subcarrier-modulated IE, PMEPR control, constant-modulus property of subcarriers, and target-steering requirement linked to OFDM waveforms. To tackle the problem, we first construct a majorization function to transform its objective function into a quadratic form. Then, we apply the consensus alternating direction method of multipliers framework to solve the reformulated problem via iterations, wherein an augmented Lagrangian is elaborated. Closed-form solutions are obtained at each iteration, whose performances are verified by comprehensive simulations.**

***Index Terms*—Information embedding, joint transmit waveform and receive filter design, orthogonal frequency division multiplexing, radar-communications, signal-to-interference-plus-noise ratio.**

I. Introduction

The joint radar and communications (JRC), [1], [2], which aims to tackle the issues of radio-frequency spectrum congestion and contention, has become a hot topic in recent years. Two major implementation ways including co-habitation [3] and co-design [4]–[14] between radar and communications have been developed for the JRC over the past several years. The former emphasizes on avoiding interference between radar and communication systems, while the latter integrates radar and communication functions into one platform to reduce size, cost, and power consumption. For the co-design that attracts significant interest, many approaches which embed information into radar emissions via orthogonal frequency division multiplexing (OFDM) [5]–[11], frequency-hopping [12], or polyphase-coded [13], [14] waveform modulations have been studied.

In the context of JRC with OFDM waveform transmission, the co-designed system typically shows robustness to multi-path effects for communications and can enable high-quality detection for radar [5]. Therefore, it has been studied extensively. The relevant work includes minimizing peak-to-mean envelope power ratio (PMEPR) or peak-to-average power ratio (PAPR) of OFDM waveform(s) [7], [8], minimizing the weighted sum of multi-user interference energy and waveform similarities [9], maximizing signal-to-interference-plus-noise ratio (SINR) or mutual information at radar [10], [11], etc. Therein lie the low-PMEPR/PAPR designs, which can help to instruct the reduction of hardware resources. They have already become the focus of the recent research.

When the JRC resides on an airborne platform, the aforementioned designs fail to cope with the issues caused by clutter and jamming, which requires the usage of space-time adaptive processing techniques to obtain good SINR performance for the radar side [14]–[19]. For the airborne JRC, the OFDM waveform transmission with frequency diversities indeed has potential to further improve performance with respect to different aspects, which necessitates the proper joint design of spatial-temporal transmission with OFDM waveform(s) and receiver adaptive filter. Unfortunately, existing works mainly focus on the single-waveform case for the traditional phased-array radar system [18], [19]. For the joint MIMO radar and communications (JMRC) with multi-OFDM waveforms leading to more challenge, there seldom exist studies in public literature.

In this paper, we study the problem of jointly designing spatial-temporal transmission with multi-OFDM waveforms and minimum variance distortionless response (MVDR) type receive filter for the airborne JMRC. Our major goal is to achieve good SINR performance for radar while ensuring accurate information embedding (IE) via the modulated OFDM waveforms with reasonable PMEPR for the communications. To achieve this goal, we first build an appropriate model that incorporates all subcarrier-related characteristics of multi-OFDM waveforms. Then, we maximize the output SINR of JMRC under constraints on IE, PMEPR control, constant-modulus property of subcarriers, and target-steering require-

This work was supported in part by the National Natural Science Foundation of China (NSFC) under grants 62271054, 62171029, and U21A20456.

ment associated with the OFDM waveforms. The joint design is formulated as a non-convex optimization problem, for which we develop an efficient algorithm to address. To achieve this, we utilize the majorization-minimization (MM) technique to transform its objective function into a quadratic form, and reformulate the newly obtained problem into a form that obeys the framework of consensus alternating direction method of multipliers (ADMM). Our remaining work is to elaborate an augmented Lagrangian for the consensus-ADMM, which helps us to obtain closed-form solutions for iterations. Simulation results verify the effectiveness of our proposed design and its superiority over existing methods.

Notations: We use $\otimes$, $\odot$, $|\cdot|$, $\|\cdot\|$, $\|\cdot\|_\infty$ $(\cdot)^{\mathrm{T}}$, $(\cdot)^{\mathrm{H}}$, $\mathbb{E}\{\cdot\}$, $\Re(\cdot)$, $\arg(\cdot)$, $\mathfrak{D}\{\cdot\}$, and $\mathrm{tr}\{\cdot\}$ to denote the Kronecker product, Hadamard product, modulus, Euclidean norm, infinity norm, transpose, Hermitian transpose, expectation, real part, argument of a complex value, diagonalization, and matrix trace, respectively. Moreover, $[\cdot]_{p,k}$ denotes the (p,k)-th element of a matrix, $\mathbf{1}_K$ is the $K\times 1$ vector with all elements equal to 1, and $\mathbf{I}_K$ stands for a $K\times K$ identity matrix.

II. Signal Model

We consider an airborne JMRC system that simultaneously performs both functions of radar and communications, which is equipped with M transmit and N receive antennas. We assume that M OFDM waveforms with each composed of K subcarriers are launched from the M antennas independently. In addition, at each transmit antenna, a burst of L pulses is emitted. We denote Δ_{f} as the subcarrier spacing in the frequency domain. Sampling via the proper interval $T_{\mathrm{s}} \triangleq 1/(K\Delta_{\mathrm{f}})$, the signal component related to the k-th subcarrier within the l-th pulse for the m-th baseband OFDM waveform can be expressed as

$$s_{m,l,k}(p) = u_{m,l,k}\exp\{j\varphi_k(p)\},\ p\in\{1,...,K\} \tag{1}$$

where p is the sampling index, $u_{m,l,k}$ is the complex weight with unit modulus of the k-th subcarrier within the l-th pulse for the m-th waveform, and $\varphi_k(p) \triangleq 2\pi(k-1)\Delta_{\mathrm{f}}(p-1)T_{\mathrm{s}}$.

For the radar side in the JMRC system, a high SINR at the output is expected. To this end, we first need to build an appropriate model. To exploit the frequency diversity gain provided by OFDM waveforms, the model incorporates the response characteristics of different subcarriers across multiple waveforms and pulses to the moving target and clutter patches. We denote $\bar{f}_k^{(\mathrm{t})}$ and $\hat{f}_k^{(\mathrm{t})}$ as the normalized Doppler and spatial frequencies of the target associated with the k-th subcarrier, respectively. Hence, the target echo at the n-th receive antenna after demodulating to the baseband can be expressed as

$$\widetilde{y}_{n,l}^{(\mathrm{t})}(p) = \sum_{m=1}^{M}\sum_{k=1}^{K}\alpha_k^{(\mathrm{t})}s_{m,l,k}(p)\exp\big\{j2\pi(l-1)\bar{f}_k^{(\mathrm{t})}\big\} \times\exp\big\{j2\pi(m-1)\hat{f}_k^{(\mathrm{t})}\big\}\exp\big\{j2\pi(n-1)\hat{f}_k^{(\mathrm{t})}\big\},\ p\in\{1,...,K\} \tag{2}$$

where $\alpha_k^{(\mathrm{t})}$ denotes the complex reflection coefficient associated with the target, describing the propagation and backscattering environments (such as attenuation, time delay, etc.) related to the k-th subcarrier.

Let us denote the Doppler, transmit, and receive steering vectors associated with the k-th subcarrier by $\mathbf{d}(\bar{f}_k^{(\mathrm{t})}) \in \mathbb{C}^{L\times 1}$, $\mathbf{a}(\hat{f}_k^{(\mathrm{t})}) \in \mathbb{C}^{M\times 1}$, and $\mathbf{b}(\hat{f}_k^{(\mathrm{t})}) \in \mathbb{C}^{N\times 1}$, respectively. Substituting (1) into (2), and also introducing the vectors $\widetilde{\mathbf{y}}_l^{(\mathrm{t})}(p) \triangleq [\widetilde{y}_{1,l}^{(\mathrm{t})}(p),...,\widetilde{y}_{N,l}^{(\mathrm{t})}(p)]^{\mathrm{T}} \in \mathbb{C}^{N\times 1}$ and $\mathbf{u}_{l,k} \triangleq [u_{1,l,k},...,u_{M,l,k}]^{\mathrm{T}} \in \mathbb{C}^{M\times 1}$, we can rewrite (2) as the vector form given as follows

$$\widetilde{\mathbf{y}}^{(\mathrm{t})}(p) = \sum_{k=1}^{K}\alpha_k^{(\mathrm{t})}\exp\{j\varphi_k(p)\}\mathfrak{D}\{\mathbf{d}(\bar{f}_k^{(\mathrm{t})})\} \otimes\mathbf{b}(\hat{f}_k^{(\mathrm{t})})\otimes\mathbf{a}^{\mathrm{T}}(\hat{f}_k^{(\mathrm{t})})\mathbf{u}_k,\ p\in\{1,...,K\} \tag{3}$$

where $\widetilde{\mathbf{y}}^{(\mathrm{t})}(p) \triangleq [(\widetilde{\mathbf{y}}_1^{(\mathrm{t})}(p))^{\mathrm{T}},...,(\widetilde{\mathbf{y}}_L^{(\mathrm{t})}(p))^{\mathrm{T}}]^{\mathrm{T}} \in \mathbb{C}^{NL\times 1}$ and $\mathbf{u}_k \triangleq [\mathbf{u}_{1,k},...,\mathbf{u}_{L,k}]^{\mathrm{T}} \in \mathbb{C}^{ML\times 1}$.

We assume that there exist N_{c} clutter patches located at the same range as that of the target, which are statistically independent between each other. Similar to (3), the received clutter at the p-th sample can be written as

$$\widetilde{\mathbf{y}}^{(\mathrm{c})}(p) = \sum_{k=1}^{K}\sum_{i=1}^{N_{\mathrm{c}}}\alpha_{k,i}^{(\mathrm{c})}\exp\{j\varphi_k(p)\}\mathfrak{D}\{\mathbf{d}(\bar{f}_{k,i}^{(\mathrm{c})})\} \otimes\mathbf{b}(\hat{f}_{k,i}^{(\mathrm{c})})\otimes\mathbf{a}^{\mathrm{T}}(\hat{f}_{k,i}^{(\mathrm{c})})\mathbf{u}_k,\ p\in\{1,...,K\} \tag{4}$$

where $\alpha_{k,i}^{(\mathrm{c})}$, $\bar{f}_{k,i}^{(\mathrm{c})}$, and $\hat{f}_{k,i}^{(\mathrm{c})}$ are the complex reflection coefficient, normalized Doppler frequency, and spatial frequency of the i-th clutter patch associated with the k-th subcarrier, respectively.

We store all target echo vectors $\{\widetilde{\mathbf{y}}^{(\mathrm{t})}(p)\}_{p=1}^{K}$ and clutter vectors $\{\widetilde{\mathbf{y}}^{(\mathrm{c})}(p)\}_{p=1}^{K}$ into $\widetilde{\mathbf{y}}^{(\mathrm{t})} \triangleq [(\widetilde{\mathbf{y}}^{(\mathrm{t})}(1))^{\mathrm{T}},...,(\widetilde{\mathbf{y}}^{(\mathrm{t})}(K))^{\mathrm{T}}]^{\mathrm{T}} \in \mathbb{C}^{NLK\times 1}$ and $\widetilde{\mathbf{y}}^{(\mathrm{c})} \triangleq [(\widetilde{\mathbf{y}}^{(\mathrm{c})}(1))^{\mathrm{T}},...,(\widetilde{\mathbf{y}}^{(\mathrm{c})}(K))^{\mathrm{T}}]^{\mathrm{T}} \in \mathbb{C}^{NLK\times 1}$, respectively. Based on (3) and (4), the overall target echo and clutter vectors in the time domain can also be respectively expressed as

$$\widetilde{\mathbf{y}}^{(\mathrm{t})} = (\mathbf{F}^{-1}\otimes\mathbf{I}_{NL})\mathbf{T}^{(\mathrm{t})}\mathbf{u} \tag{5}$$

$$\widetilde{\mathbf{y}}^{(\mathrm{c})} = \sum_{i=1}^{N_{\mathrm{c}}}(\mathbf{F}^{-1}\otimes\mathbf{I}_{NL})\mathbf{T}_i^{(\mathrm{c})}\mathbf{u} \tag{6}$$

where $\mathbf{u} \triangleq [\mathbf{u}_1^{\mathrm{T}},...,\mathbf{u}_K^{\mathrm{T}}]^{\mathrm{T}} \in \mathbb{C}^{MLK\times 1}$, $\mathbf{F} \in \mathbb{C}^{K\times K}$ is the discrete Fourier transform (DFT) matrix whose (p,k)-th element is given by $[\mathbf{F}]_{p,k} = (1/K)\exp\{-j\varphi_k(p)\}$, $p,k\in\{1,...,K\}$, and $\mathbf{T}^{(\mathrm{t})} \in \mathbb{C}^{NLK\times MLK}$ and $\mathbf{T}_i^{(\mathrm{c})} \in \mathbb{C}^{NLK\times MLK}$ are block diagonal matrices whose k-th diagonal blocks are respectively given by

$$\mathbf{\Psi}_k^{(\mathrm{t})} \triangleq \alpha_k^{(\mathrm{t})}\mathfrak{D}\{\mathbf{d}(\bar{f}_k^{(\mathrm{t})})\}\otimes\mathbf{b}(\hat{f}_k^{(\mathrm{t})})\otimes\mathbf{a}^{\mathrm{T}}(\hat{f}_k^{(\mathrm{t})}),\ k\in\{1,...,K\} \tag{7}$$

$$\mathbf{\Psi}_{k,i}^{(\mathrm{c})} \triangleq \alpha_{k,i}^{(\mathrm{c})}\mathfrak{D}\{\mathbf{d}(\bar{f}_{k,i}^{(\mathrm{c})})\}\otimes\mathbf{b}(\hat{f}_{k,i}^{(\mathrm{c})})\otimes\mathbf{a}^{\mathrm{T}}(\hat{f}_{k,i}^{(\mathrm{c})}),\ k\in\{1,...,K\}. \tag{8}$$

Applying the DFT to (5) and (6), the target echo vector $\widetilde{\mathbf{y}}^{(\mathrm{t})}$ and clutter vector $\widetilde{\mathbf{y}}^{(\mathrm{c})}$ are converted as

$$\mathbf{y}^{(\mathrm{t})} = (\mathbf{F}\otimes\mathbf{I}_{NL})(\mathbf{F}^{-1}\otimes\mathbf{I}_{NL})\mathbf{T}^{(\mathrm{t})}\mathbf{u} = \mathbf{T}^{(\mathrm{t})}\mathbf{u} \tag{9}$$

$$\mathbf{y}^{(\mathrm{c})} = \sum_{i=1}^{N_{\mathrm{c}}}(\mathbf{F}\otimes\mathbf{I}_{NL})(\mathbf{F}^{-1}\otimes\mathbf{I}_{NL})\mathbf{T}_i^{(\mathrm{c})}\mathbf{u} = \sum_{i=1}^{N_{\mathrm{c}}}\mathbf{T}_i^{(\mathrm{c})}\mathbf{u}. \tag{10}$$

In this scenario, we also consider the barrage-noise-type jammers, and utilize the vector $\mathbf{y}^{(\mathrm{j+n})} \in \mathbb{C}^{NLK\times 1}$ to denote

the jamming plus noise vector. Therefore, the observed signal at the radar receiver can be expressed as

$$\mathbf{y} = \mathbf{y}^{(\mathrm{t})} + \mathbf{y}^{(\mathrm{c})} + \mathbf{y}^{(\mathrm{j+n})}. \tag{11}$$

For the airborne JMRC system, the adaptive filter, characterized by $\mathbf{w} \in \mathbb{C}^{NLK\times 1}$, is applied on the received signal vector (11), which leads to the SINR written as follows

$$\mathrm{SINR} = \frac{|\mathbf{w}^{\mathrm{H}}\mathbf{T}^{(\mathrm{t})}\mathbf{u}|^2}{\mathbf{w}^{\mathrm{H}}(\mathbf{R}_{\mathrm{c}}+\mathbf{R}_{\mathrm{j+n}})\mathbf{w}} \tag{12}$$

where $\mathbf{R}_{\mathrm{c}} \triangleq \mathbb{E}\{\mathbf{y}^{(\mathrm{c})}(\mathbf{y}^{(\mathrm{c})})^{\mathrm{H}}\} = \sum_{i=1}^{N_{\mathrm{c}}} \mathbf{T}_i^{(\mathrm{c})}\mathbf{u}\mathbf{u}^{\mathrm{H}}(\mathbf{T}_i^{(\mathrm{c})})^{\mathrm{H}}$, and $\mathbf{R}_{\mathrm{j+n}} \in \mathbb{C}^{NLK\times NLK}$ is the covariance matrix related to $\mathbf{y}^{(\mathrm{j+n})}$.

For the communication side in the JMRC system, we embed information into the weights of partial subcarriers via phase shift keying (PSK) modulations. We introduce $\mathbf{z} \in \mathbb{R}^{MLK\times 1}$ to record the indices of modulated subcarriers, and let $\mathbf{u}^{(\mathrm{d})} \in \mathbb{C}^{MLK\times 1}$ be the pre-determined weight vector which contains all the required weights at the positions indexed by $\mathbf{z}$ while otherwise enables zero elements. Then, the weight vector $\mathbf{u}$ establishes a relationship with $\mathbf{u}^{(\mathrm{d})}$ carrying information, which is expressed as $\mathbf{z} \odot \mathbf{u} = \mathbf{u}^{(\mathrm{d})}$. Typically, the accurate IE is necessary to guarantee a low symbol error rate (SER).

In addition, the low PAPR/PMEPR is also needed for the OFDM waveforms. For the given baseband signal (1), we choose PMEPR for evaluation, whose definition is given by

$$\mathrm{PMEPR} = \max_{m} \frac{\max_{p,l}\left|\sum_{k=1}^{K} s_{m,l,k}(p)\right|^2}{\sum_{l=1}^{L}\sum_{p=1}^{K}\left|\sum_{k=1}^{K} s_{m,l,k}(p)\right|^2/(LK)}, \quad m \in \{1,...,M\}. \tag{13}$$

III. Joint Design of Multi-OFDM Waveforms and Receive Adaptive Filter

Based on the signal model presented in the previous section, we consider to increase the output SINR of the adaptive filter, and meanwhile, to guarantee the accurate IE and reasonable PMEPR performance of OFDM waveforms. To this end, we propose a joint design of multi-OFDM waveforms and receive adaptive filter for the JMRC, which can be formulated as

$$\begin{aligned}
\max_{\mathbf{w},\mathbf{u}} \quad & \mathrm{SINR} && \text{(14a)}\\
\text{s.t.} \quad & |\mathbf{w}^{\mathrm{H}}\mathbf{T}^{(\mathrm{t})}\mathbf{u}| = 1 && \text{(14b)}\\
& |\mathbf{u}(q)| = 1,\ \forall q \in \{1,...,MLK\} && \text{(14c)}\\
& \mathbf{z} \odot \mathbf{u} = \mathbf{u}^{(\mathrm{d})} && \text{(14d)}\\
& \mathrm{PMEPR} \le \delta && \text{(14e)}
\end{aligned}$$

where δ is a parameter that defines the maximum acceptable PMEPR. Note that the constraint (14c) guarantees the constant-modulus property of weights associated with subcarriers.

The formulated optimization problem (14) is non-convex. To solve it, we first fix $\mathbf{u}$, and rewrite it as an MVDR optimization problem with respect to $\mathbf{w}$, whose solution is given by

$$\mathbf{w} = \frac{(\mathbf{R}_{\mathrm{c}}+\mathbf{R}_{\mathrm{j+n}})^{-1}\mathbf{T}^{(\mathrm{t})}\mathbf{u}}{\mathbf{u}^{\mathrm{H}}(\mathbf{T}^{(\mathrm{t})})^{\mathrm{H}}(\mathbf{R}_{\mathrm{c}}+\mathbf{R}_{\mathrm{j+n}})^{-1}\mathbf{T}^{(\mathrm{t})}\mathbf{u}}. \tag{15}$$

Substituting (15) into (12), the SINR can be rewritten as

$$\mathrm{SINR} = \mathbf{u}^{\mathrm{H}}(\mathbf{T}^{(\mathrm{t})})^{\mathrm{H}}(\mathbf{R}_{\mathrm{c}} + \mathbf{R}_{\mathrm{j+n}})^{-1}\mathbf{T}^{(\mathrm{t})}\mathbf{u}. \tag{16}$$

Then, the next stage is to solve the problem with respect to $\mathbf{u}$ given as follows

$$\begin{aligned}
\min_{\mathbf{u}} \quad & -\mathbf{u}^{\mathrm{H}}(\mathbf{T}^{(\mathrm{t})})^{\mathrm{H}}(\mathbf{R}_{\mathrm{c}} + \mathbf{R}_{\mathrm{j+n}})^{-1}\mathbf{T}^{(\mathrm{t})}\mathbf{u} && \text{(17a)}\\
\text{s.t.} \quad & |\mathbf{u}(q)| = 1,\ \forall q \in \{1,...,MLK\} && \text{(17b)}\\
& \mathbf{z} \odot \mathbf{u} = \mathbf{u}^{(\mathrm{d})} && \text{(17c)}\\
& \mathrm{PMEPR} \le \delta && \text{(17d)}
\end{aligned}$$

which is also non-convex and difficult to be solved.

Before proceeding with (17), we need to derive the objective function (17a) and constraint (17d) into proper forms, so that the problem (17) can be solved. To this end, we utilize the MM technique to majorize the objective function (17a) [20], which leads to the majorant given as follows

$$\begin{aligned}
g(\mathbf{u},\mathbf{u}^{(v)}) = {} & \mathrm{tr}\big\{(\mathbf{\Omega}^{(v)})^{-1}\mathbf{T}^{(\mathrm{t})}\mathbf{u}^{(v)}(\mathbf{T}^{(\mathrm{t})}\mathbf{u}^{(v)})^{\mathrm{H}}(\mathbf{\Omega}^{(v)})^{-1}\mathbf{\Omega}\big\}\\
& - 2\Re\big\{(\boldsymbol{\beta}^{(v)})^{\mathrm{H}}\mathbf{u}\big\} + \mathrm{const}
\end{aligned} \tag{18}$$

where we utilize the superscript $(\cdot)^{(v)}$ to mark the corresponding updates at the v-th iteration, $\boldsymbol{\beta}^{(v)} \triangleq (\mathbf{T}^{(\mathrm{t})})^{\mathrm{H}}(\mathbf{\Omega}^{(v)})^{-1} \times \mathbf{T}^{(\mathrm{t})}\mathbf{u}^{(v)}$, and $\mathbf{\Omega} \triangleq \mathbf{R}_{\mathrm{c}} + \mathbf{R}_{\mathrm{j+n}}$. Substituting $\mathbf{R}_{\mathrm{c}} = \sum_{i=1}^{N_{\mathrm{c}}} \mathbf{T}_i^{(\mathrm{c})}\mathbf{u}\mathbf{u}^{\mathrm{H}}(\mathbf{T}_i^{(\mathrm{c})})^{\mathrm{H}}$ into (18) and utilizing the properties of the trace operation, we can rewrite the majorant (18) as

$$g(\mathbf{u},\mathbf{u}^{(v)}) = \mathbf{u}^{\mathrm{H}}\mathbf{\Phi}^{(v)}\mathbf{u} - 2\Re\big\{(\boldsymbol{\beta}^{(v)})^{\mathrm{H}}\mathbf{u}\big\} + \mathrm{const} \tag{19}$$

where $\mathbf{\Phi}^{(v)} \triangleq \sum_{i=1}^{N_{\mathrm{c}}}(\mathbf{T}_i^{(\mathrm{c})})^{\mathrm{H}}(\mathbf{\Omega}^{(v)})^{-1}\mathbf{T}^{(\mathrm{t})}\mathbf{u}^{(v)}(\mathbf{u}^{(v)})^{\mathrm{H}}(\mathbf{T}^{(\mathrm{t})})^{\mathrm{H}} \times (\mathbf{\Omega}^{(v)})^{-1}\mathbf{T}_i^{(\mathrm{c})}$.

To tackle the constraint (17d), we introduce the OFDM waveform vector $\mathbf{s} \in \mathbb{C}^{MLK\times 1}$ whose q-th element is given by $\mathbf{s}(q) \triangleq \sum_{k=1}^{K} s_{m,l,k}(p),\ q = (p-1)ML + (l-1)M + m, q \in \{1,...,MLK\}$. Then, the baseband OFDM signal in (1) can also be expressed as $\mathbf{s} = (\mathbf{F}\otimes\mathbf{I}_{ML})\mathbf{u}$, and the PMEPR in (13) can be rewritten as $\mathrm{PMEPR} = \frac{\|\mathbf{s}\|_\infty^2}{\|\mathbf{s}\|^2/(MLK)}$. Since $\|\mathbf{s}\|^2/(MLK) = K$, we can transform (17d) into

$$\left|\mathbf{e}_q^{\mathrm{T}}(\mathbf{F}\otimes\mathbf{I}_{ML})\mathbf{u}\right|^2 \le \delta K,\ \forall q \in \{1,...,MLK\} \tag{20}$$

where $\mathbf{e}_q \in \mathbb{C}^{MLK\times 1}$ is a standard unit vector whose q-th element equals 1.

Utilizing (19) and (20), and ignoring the constant term, we can express the majorized optimization problem for (17) as

$$\begin{aligned}
\min_{\mathbf{u}} \quad & \mathbf{u}^{\mathrm{H}}\mathbf{\Phi}^{(v)}\mathbf{u} - 2\Re\big\{(\boldsymbol{\beta}^{(v)})^{\mathrm{H}}\mathbf{u}\big\} && \text{(21a)}\\
\text{s.t.} \quad & |\mathbf{u}(q)| = 1,\ \forall q \in \{1,...,MLK\} && \text{(21b)}\\
& \mathbf{z} \odot \mathbf{u} = \mathbf{u}^{(\mathrm{d})} && \text{(21c)}\\
& \left|\mathbf{e}_q^{\mathrm{T}}(\mathbf{F}\otimes\mathbf{I}_{ML})\mathbf{u}\right|^2 \le \delta K,\ \forall q \in \{1,...,MLK\}. && \text{(21d)}
\end{aligned}$$

To solve (21), we introduce virtual auxiliary variables $\mathbf{x}_q \in \mathbb{C}^{MLK\times 1},\ q = 1,...,MLK$ to reformulate it as

$$\begin{aligned}
\min_{\mathbf{u},\{\mathbf{x}_q\}_{q=1}^{MLK}} \quad & \mathbf{u}^{\mathrm{H}}\mathbf{\Phi}^{(v)}\mathbf{u} - 2\Re\big\{(\boldsymbol{\beta}^{(v)})^{\mathrm{H}}\mathbf{u}\big\} && \text{(22a)}\\
\text{s.t.} \quad & \mathbf{u} = \mathbf{x}_q,\ \forall q \in \{1,...,MLK\} && \text{(22b)}\\
& \mathbf{z} \odot \mathbf{u} = \mathbf{u}^{(\mathrm{d})} && \text{(22c)}\\
& |\mathbf{u}(q)| = 1,\ \forall q \in \{1,...,MLK\} && \text{(22d)}\\
& \left|\mathbf{e}_q^{\mathrm{T}}(\mathbf{F}\otimes\mathbf{I}_{ML})\mathbf{x}_q\right|^2 \le \delta K,\ \forall q \in \{1,...,MLK\} && \text{(22e)}
\end{aligned}$$

Algorithm 1 Joint design for JMRC.

1: Initialization: $v \leftarrow 0$, $\mathbf{u}^{(0)}$, $\mathbf{x}_q^{(0)}$, $\boldsymbol{\lambda}_q^{(0)}$, $q \in \{1, ..., MLK\}$
2: **repeat**
3: Calculate $\mathbf{u}^{(v+1)}$, $\mathbf{x}_q^{(v+1)}$, and $\boldsymbol{\lambda}_q^{(v+1)}$, $\forall q$ via (24)–(26)
4: $v \leftarrow v + 1$
5: **until** convergence
6: Calculate $\mathbf{w}$ via (15)

which allows for the application of consensus-ADMM for finding solutions [21]. To this end, we construct the augmented Lagrangian for (22) given by

$$\mathcal{L}\big(\mathbf{u}, \mathbf{x}_q, \boldsymbol{\lambda}_q\big) = \mathbf{u}^{\mathrm{H}}\boldsymbol{\Phi}^{(v)}\mathbf{u} - 2\Re\big\{(\boldsymbol{\beta}^{(v)})^{\mathrm{H}}\mathbf{u}\big\} + \rho\sum_{q=1}^{MLK}\|\mathbf{x}_q - \mathbf{u} + \boldsymbol{\lambda}_q\|^2 - \rho\sum_{q=1}^{MLK}\|\boldsymbol{\lambda}_q\|^2 \quad (23)$$

where $\boldsymbol{\lambda}_q \in \mathbb{C}^{MLK\times 1}$, $q = 1, ..., MLK$ are Lagrange multipliers, and ρ is the penalty parameter. The resulting ADMM procedures consist of the updates given as follows

$$\mathbf{u}^{(v+1)} = \mathbf{u}^{(\mathrm{d})} + (\mathbf{1}_{MLK} - \mathbf{z}) \odot \exp\left\{j \cdot \arg\left(\left(\boldsymbol{\Phi}^{(v)} + MLK\rho\mathbf{I}_{MLK}\right)^{-1}\left(\boldsymbol{\beta}^{(v)} + \rho\sum_{q=1}^{MLK}\left(\mathbf{x}_q^{(v)} + \boldsymbol{\lambda}_q^{(v)}\right)\right)\right)\right\} \quad (24)$$

$$\mathbf{x}_q^{(v+1)} = \begin{cases} \mathbf{u}^{(v+1)} - \boldsymbol{\lambda}_q^{(v)}, & \text{if } \left|\boldsymbol{\gamma}_q^{\mathrm{H}}(\mathbf{u}^{(v+1)} - \boldsymbol{\lambda}_q^{(v)})\right|^2 \le \delta K, \\ & q \in \{1, ..., MLK\} \\ \mathbf{u}^{(v+1)} - \boldsymbol{\lambda}_q^{(v)} + \dfrac{\sqrt{\delta K} - |\boldsymbol{\gamma}_q^{\mathrm{H}}(\mathbf{u}^{(v+1)} - \boldsymbol{\lambda}_q^{(v)})|}{\|\boldsymbol{\gamma}_q\|^2 |\boldsymbol{\gamma}_q^{\mathrm{H}}(\mathbf{u}^{(v+1)} - \boldsymbol{\lambda}_q^{(v)})|} \\ \quad \times \boldsymbol{\gamma}_q\boldsymbol{\gamma}_q^{\mathrm{H}}(\mathbf{u}^{(v+1)} - \boldsymbol{\lambda}_q^{(v)}), & \text{otherwise} \end{cases} \quad (25)$$

$$\boldsymbol{\lambda}_q^{(v+1)} = \boldsymbol{\lambda}_q^{(v)} + \mathbf{x}_q^{(v+1)} - \mathbf{u}^{(v+1)}, \ q \in \{1, ..., MLK\} \quad (26)$$

where $\boldsymbol{\gamma}_q \triangleq (\mathbf{F}^{\mathrm{H}} \otimes \mathbf{I}_{ML})\mathbf{e}_q \in \mathbb{C}^{MLK\times 1}$, $\forall q \in \{1, ...MLK\}$. Note that (24) and (25) are obtained via solving the relevant non-convex optimization and projection problems, respectively, which enables a lower computational complexity than the existing approaches via the non-linear equality constrained ADMM and free optimization solver [9], [14]. The detailed derivations to (24)–(26) are omitted to show due to the space limitation.

Returning to (14), the overall procedures are summarized in Algorithm 1. Note that Algorithm 1 can guarantee convergence after a certain number of iterations due to the property of the MM framework [20] and the fact that consensus-ADMM converges to a Karush-Kuhn-Tucker point [21].

IV. Simulation Results

We evaluate the performances of our proposed design, and compare it with existing works which include [6] and [14]. Throughout the simulations, we assume that the airborne platform is flying at a fixed height. In the considered scenario, there exist $N_{\mathrm{c}} = 5$ clutter patches on the ground. Moreover,

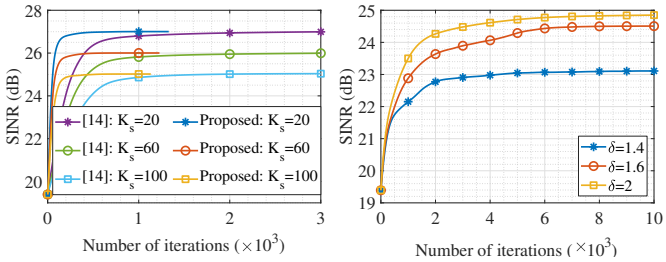

(a) Convergence speed versus K_{s}. (b) Convergence speed versus δ.

Fig. 1. Evaluations and comparisons on convergence speed.

TABLE I
Evaluations and Comparisons on SINR Performance.

	$\delta=1.4$			$\delta=1.6$			$\delta=2$		
	$K_{\mathrm{s}}=20$	$K_{\mathrm{s}}=60$	$K_{\mathrm{s}}=100$	$K_{\mathrm{s}}=20$	$K_{\mathrm{s}}=60$	$K_{\mathrm{s}}=100$	$K_{\mathrm{s}}=20$	$K_{\mathrm{s}}=60$	$K_{\mathrm{s}}=100$
[6]	20.07	19.02	17.33	20.08	19.33	18.37	20.09	19.54	18.79
Proposed	26.88	25.59	23.39	26.90	25.82	24.44	26.95	25.93	24.80

we set the signal-to-noise ratio for radar to be 20 dB, while the clutter-to-noise ratio is fixed at 27 dB. Unless otherwise specified, we always utilize BPSK modulation to embed communication symbols into $K_{\mathrm{s}} \triangleq \mathbf{z}^{\mathrm{T}}\mathbf{1}_{MLK}$ subcarrier weights, where K_{s} is used to denote the number of weights pre-determined by $\mathbf{u}^{(\mathrm{d})}$. Other parameters include $\Delta_{\mathrm{f}} = 10$ MHz, $M = 4$, $N = 2$, $K = 10$, and $L = 5$. We choose the absolute difference of the SINR values obtained at the current and previous iterations normalized by the initial one as the stopping criterion, whose tolerance is set to be 10^{-7}.

In the first example, we evaluate the SINR performance of our proposed algorithm versus the numbers of iterations for different cases of the pre-determined weight number characterized by K_{s}, wherein the parameter δ is fixed to 5. We also evaluate the SINR performance versus the numbers of iterations for different cases of the parameter δ characterizing the maximum acceptable PMEPR level, wherein $K_{\mathrm{s}} = 100$ is tested. In addition, we compare the former with the algorithm involving 'MM-neADMM' [14]. The corresponding results for varying $K_{\mathrm{s}} \in \{20, 60, 100\}$ and $\delta \in \{1.4, 1.6, 2\}$ are shown in Fig. 1(a) and Fig. 1(b), respectively. It can be seen from Fig. 1(a) that our proposed algorithm consistently shows a better convergence speed compared to [14] in all tested scenarios. Our algorithm costs a smaller number of iterations to implement a high SINR than [14]. Moreover, it can also be seen from Fig. 1 that the optimization effect on SINR is better when K_{s} reduces or δ increases.

In the second example, we evaluate the SINR performances of the proposed design obtained using the conventional model of [6] and our developed model. The former ignores the differences in Doppler and spatial frequencies associated with varying subcarriers. Here, the maximum acceptable PMEPR δ and the number of pre-determined subcarriers K_{s} are chosen from the sets $\{1.4, 1.6, 2\}$ and $\{20, 60, 100\}$, respectively. The obtained average SINR values (in dBs) over 30 independent trials are shown in Table I. It can be seen that the SINR values associated with our model are larger than those of [6] in all

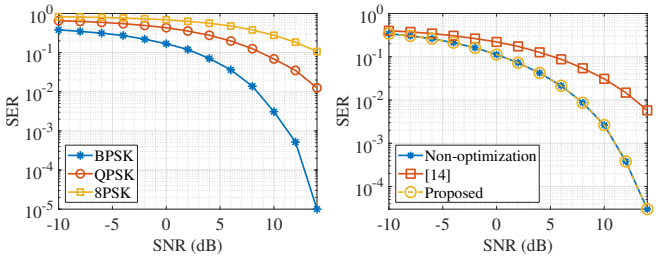

(a) SER for different modulations. (b) SER for different methods.

Fig. 2. Evaluations and comparisons on SER performance.

tested cases. For example, when $K_{\mathrm{s}} = 20$ and $\delta = 1.4$ are experimented, the obtained SINR value has been increased by 6.81 dB. In addition, it can also be seen from Table I that the SINR value with smaller K_{s} (or larger δ) is less sensitive to δ (or K_{s}). The reason lies in the larger degrees of freedom for the joint design enabled by smaller K_{s} or larger δ.

In the third example, we evaluate the SER performance of the proposed design in terms of different modulations which include BPSK, QPSK, and 8PSK schemes. In the case of BPSK modulation, we also compare the SER performance for the waveforms generated by our proposed design with those produced by other methods including the non-optimization way and similarity-constrained design in [14]. We set $K_{\mathrm{s}} = 100$ for all tested methods, and set $\delta = 2$ for our design. The corresponding results over 1000 Monte Carlo experiments are shown in Fig. 2. It can be seen from Fig. 2(a) that the SER performance increases when the tested signal-to-noise ratio (SNR) value increases, and the case associated with BPSK shows the best overall SER performance. Therefore, our design can support information transmission via IE. It can also be seen from Fig. 2(b) that our proposed method has the same SER performance as the non-optimization approach, and it enables the better SER performance than [14]. In the case of a 10 dB SNR, the obtained SER value has been reduced by 0.028. Therefore, our optimization design can guarantee an accurate IE.

V. Conclusion

We have proposed the joint design of spatial-temporal transmission with OFDM waveforms and receive adaptive filter in the context of airborne JMRC, which aims to increase SINR at the radar receiver, and meanwhile to guarantee accurate IE and low PMEPR. To this end, we first have built an appropriate model that incorporates all subcarrier-related characteristics of multi-OFDM waveforms. Then, we have proposed a design that maximizes the SINR under the constraints on accurate IE, acceptable PMEPR, constant-modulus property, and target-steering requirement, which has been formulated as a non-convex optimization problem. To solve it, we have exploited the MM techniques followed by the consensus-ADMM to obtain the closed-form solution at each iteration, whose performances have been verified by comprehensive simulations.

References

[1] H. Griffiths, L. Cohen, S. Watts, C. Baker, M. Wicks, and S. Blunt, "Radar spectrum engineering and management: Technical and regulatory issues," *Proc. IEEE*, vol. 103, no. 1, pp. 85–102, Jan. 2014.

[2] K. V. Mishra, M. R. Bhavani Shankar, V. Koivunen, B. Ottersten, and S. A. Vorobyov, "Toward millimeter-wave joint radar communications: A signal processing perspective," *IEEE Signal Process. Mag.*, vol. 36, no. 5, pp. 100–114, Sep. 2019.

[3] A. Aubry, A. De Maio, M. Piezzo, and A. Farina, "Radar waveform design in a spectrally crowded environment via nonconvex quadratic optimization," *IEEE Trans. Aerosp. Electron. Syst.*, vol. 50, no. 2, pp. 1138–1152, Apr. 2014.

[4] A. Hassanien, M. G. Amin, Y. D. Zhang, and F. Ahmad, "Dual-function radar-communications: Information embedding using sidelobe control and waveform diversity," *IEEE Trans. Signal Process.*, vol. 64, no. 8, pp. 2168–2181, Apr. 2016.

[5] C. Sturm and W. Wiesbeck, "Waveform design and signal processing aspects for fusion of wireless communications and radar sensing," *Proc. IEEE*, vol. 99, no. 7, pp. 1236–1259, Jul. 2011.

[6] Y. L. Sit, B. Nuss, and T. Zwick, "On mutual interference cancellation in a MIMO OFDM multiuser radar-communication network," *IEEE Trans. Veh. Technol.*, vol. 67, no. 4, pp. 3339–3348, Apr. 2018.

[7] X. Xu, Y. Li, R. Tao, and T. Shan, "OFDM waveform design with good correlation level and peak-to-mean envelope power ratio for the joint MIMO radar and communications," in *Proc. IEEE Int. Conf. Acoust., Speech, Signal Process. (ICASSP)*, Seoul, Korea, Republic of, Apr. 2024, pp. 8776–8780.

[8] Y. Huang, S. Hu, S. Ma, Z. Liu, and M. Xiao, "Designing low-PAPR waveform for OFDM-based RadCom systems," *IEEE Trans. Wireless Commun.*, vol. 21, no. 9, pp. 6979–6993, Sep. 2022.

[9] X. Hu, C. Masouros, F. Liu, and R. Nissel, "Low-PAPR DFRC MIMO-OFDM waveform design for integrated sensing and communications," in *Proc. IEEE Int. Conf. Commun.*, Seoul, Korea, Republic of, May 2022, pp. 1599–1604.

[10] F. Wang and H. Li, "Power allocation for coexisting multicarrier radar and communication systems in cluttered environments," *IEEE Trans. Signal Process.*, vol. 69, pp. 1603–1613, Feb. 2021.

[11] Z. Wei, J. Piao, X. Yuan, H. Wu, J. A. Zhang, Z. Feng, L. Wang, and P. Zhang, "Waveform design for MIMO-OFDM integrated sensing and communication system: An information theoretical approach," *IEEE Trans. Commun.*, vol. 72, no. 1, pp. 496–509, Jan. 2024.

[12] W. Baxter, E. Aboutanios, and A. Hassanien, "Joint radar and communications for frequency-hopped MIMO systems," *IEEE Trans. Signal Process.*, vol. 70, pp. 729–742, Jan. 2022.

[13] Y. Li, X. Wu, and R. Tao, "Waveform design for the joint MIMO radar and communications with low integrated sidelobe levels and accurate information embedding," in *Proc. IEEE Int. Conf. Acoust., Speech, Signal Process. (ICASSP)*, Toronto, ON, Canada, Jun. 2021, pp. 8263–8267.

[14] R. Liu, M. Li, Q. Liu, and A. L. Swindlehurst, "Joint waveform and filter designs for STAP-SLP-based MIMO-DFRC systems," *IEEE J. Sel. Areas Commun.*, vol. 40, no. 6, pp. 1918–1931, Jun. 2022.

[15] J. Li, P. Stoica, and X. Zheng, "Signal synthesis and receiver design for MIMO radar imaging," *IEEE Trans. Signal Process.*, vol. 56, no. 8, pp. 3959–3968, Aug. 2008.

[16] L. Wu, P. Babu, and D. P. Palomar, "Transmit waveform/receive filter design for MIMO radar with multiple waveform constraints," *IEEE Trans. Signal Process.*, vol. 66, no. 6, pp. 1526–1540, Mar. 2018.

[17] B. Tang and J. Tang, "Joint design of transmit waveforms and receive filters for MIMO radar space-time adaptive processing," *IEEE Trans. Signal Process.*, vol. 64, no. 18, pp. 4707–4722, Sep. 2016.

[18] S. Sen, "OFDM radar space-time adaptive processing by exploiting spatio-temporal sparsity," *IEEE Trans. Signal Process.*, vol. 61, no. 1, pp. 118–130, Jan. 2013.

[19] S. Sen, "PAPR-constrained Pareto-optimal waveform design for OFDM-STAP radar," *IEEE Trans. Geosci. Remote Sens.*, vol. 52, no. 6, pp. 3658–3669, Jun. 2014.

[20] D. R. Hunter and K. Lange, "A tutorial on MM algorithms," *The American Statistician*, vol. 58, no. 1, pp. 30–37, 2004.

[21] K. Huang and N. D. Sidiropoulos, "Consensus-ADMM for general quadratically constrained quadratic programming," *IEEE Trans. Signal Process.*, vol. 64, no. 20, pp. 5297–5310, Oct. 2016.